THE JOURNAL OF PHYSICAL CHEMISTRY C

Article

Cite This: J. Phys. Chem. C 2019, 123, 21548−21553

pubs.acs.org/JPCC

Metal-Free Activation of N_2 by Persistent Carbene Pairs: An Ab Initio Investigation

Shahriar N. Khan,[†] Apostolos Kalemos,*[,‡] and Evangelos Miliordos*[,†]

[†]Department of Chemistry and Biochemistry, Auburn University, Auburn, Alabama 36849-5312, United States

[‡]Department of Chemistry, Laboratory of Physical Chemistry, National and Kapodistrian University of Athens, Athens 15771, Greece

Supporting Information

ABSTRACT: A metal-free activation process of dinitrogen is reported based on its reaction with two persistent (stable) carbenes. To analyze the reaction mechanism, we first employed methylene as the simplest representative. Potential energy profiles for every reaction step reveal that the reaction proceeds via the formation of an intermediate diazoalkane. The subsequent attack of second methylene facilitates the rupture of the two π-bonds of N_2 replacing them with π-bonds between carbon and nitrogen. This synergistic attack mimics the action of frustrated Lewis pairs with enhanced activity because of the dual chemical behavior of each carbene, being a Lewis acid and base at the same time. The reported energy landscape for a persistent $((CH_3)_3C)_2C$ carbene pair represents a model case, where the carbene dimerization is less favorable than N_2 activation. The present theoretical work introduces the notion of chemical bond activation by persistent carbene pairs. Future work will explore the possibility of activating other molecules with smaller energy barriers by tuning the electronic and geometric properties of the involved carbene.

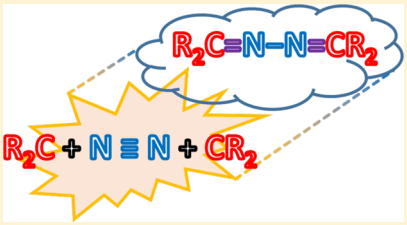

1. INTRODUCTION

Carbon, nitrogen, and oxygen are the main building blocks of all forms of life. Earth's atmosphere serves as a reservoir of nitrogen (78% abundance), from where it can be introduced into organic compounds with the help of a few microorganisms. N_2 has one of the strongest chemical bonds rendering its activation a challenging task for industrial applications. Triple-bonded $N_2(X^1\Sigma_g^+)$ has a binding energy D_0 of 9.7594 eV or 225.05 kcal/mol.[1] From the electronic structure viewpoint, the ground state of N_2 is well separated from its excited states, which excludes the possibility of their involvement in the activation process.[2] The first excited state is $^3\Sigma_u^+$ 50 203.63 cm^{-1} (=143.54 kcal/mol) higher in energy and practically inaccessible. Both factors (large D_0 and high excitation energies) render N_2 highly unreactive. Current approaches to activate N_2 include biomimetic (enzyme driven) and catalytic (metal catalyst) routes such as the energy demanding Haber−Bosch process.[3−11]

A relatively new concept is the metal-free activation of small molecules by using frustrated Lewis pairs (FLP).[12−14] It is a modification of acid−base conjugation, where steric factors prevent the Lewis acid−base couple from their association. The two separate active sites of this separated acid−base pair function as a "tug-of-war" game and are potent to cleave chemical bonds such as H_2, CO_2, and the C−C ethylene bond.[15−17] The metal-free activation of the triple-bonded N_2 is still elusive.[8]

In this work, we report metal-free N_2 activation by using a carbene pair. The idea of activating chemical bonds with a single carbene has been documented in the literature,[16,18,19] and the present report extends this very same idea to a carbene pair. Single or pairs of boron compounds with a similar structure to the present carbenes has been recently reported as an alternative for the activation or separation of N_2 molecules.[20−22] Carbenes are generally very reactive, unstable, and prone to dimerization, but persistent carbenes are reluctant to such a process mainly because of their large size.[23,24] Our calculations suggest that the latent high reactivity of persistent carbenes can be used to activate the triply bonded N_2 system. In order to provide a deeper understanding of the underlying mechanism, we have investigated every single reaction step using high level theoretical computations. The electronic structure changes of each step are also monitored and represented by simple valence-bond-Lewis (vbL) diagrams.

To simplify our discussion, we initially employ the smallest possible carbene, methylene (CH_2), to study the $CH_2 + N_2 + CH_2$ reaction. A representative model of a persistent carbene, $((CH_3)_3C)_2C$, is employed later in Section 3. Section 2 describes the computational details, and our results are reported and analyzed in Section 3. Section 4 concludes our study.

2. METHODOLOGY

Multireference configuration interaction (MRCI) and coupled cluster singles, doubles, and perturbative triples (CCSD(T))

Received: May 29, 2019
Revised: August 7, 2019
Published: August 8, 2019

DOI: 10.1021/acs.jpcc.9b05124
J. Phys. Chem. C 2019, 123, 21548−21553

were employed to study the $CH_2 + N_2 + CH_2$ reaction pathway. Complete potential energy profiles (PEPs) are constructed for every reaction step at MRCI + Q (MRCI + Davidson correction) to minimize the size extensivity errors. The active space of the reference complete active space self-consistent field wave function was adjusted to compromise the computational cost and accuracy of the calculations. The inclusion of all 22 valence electrons in 20 valence orbitals was deemed impractical. Therefore, we excluded the molecular orbitals and electrons corresponding to the inert C−H bonds, resulting to an active space of 14 electrons in 12 orbitals. The dynamic correlation of all valence electrons is considered at the MRCI level.

The wave function along the PEPs revealed the single-reference nature of the stationary points (minima and transition states) and that chemical bonds are cleaved and reformed via dative bonds (donation of electron pairs from doubly occupied orbitals to vacant antibonding ones) rather than homolytic cleavage and spin recoupling. Therefore, a minimal active space with the involved molecular orbitals would suffice. Such calculations were also performed and gave PEPs the exact same morphology. Additionally, the use of the single-reference CCSD(T) and single-determinantal density functional theory (DFT) approaches is validated by the small T_1 diagnostics at the CCSD level. T_1 diagnostic values are tabulated in the Supporting Information and range from 0.007 to 0.021.

In the case of CH_2, the optimization of all molecular structures is accomplished at CCSD(T). Harmonic vibrational frequency calculations at the same level enabled us to identify stationary points as global minima or saddle points. In the $((CH_3)_3C)_2C$ case, DFT geometry optimizations were performed for both reaction intermediates and transition states. We have employed the B3LYP functional including D3 dispersion corrections. All optimized geometries and vibrational frequencies are reported in the Supporting Information section. The correlation-consistent triple-ζ cc-pVTZ basis set for all atoms is used throughout this study. The MRCI and CCSD(T) calculations are carried out with MOLPRO[25] and DFT calculations with Gaussian 16.[26]

3. RESULTS AND DISCUSSION

The sequence of the low-lying electronic states of carbenes (RCR′) depends heavily on R and R′ groups. With proper engineering, the ground state can be of either singlet or triplet spin symmetry.[27]

The ground state of CH_2 is of triplet spin symmetry ($\tilde{X}^3B_1$) followed by three singlets ($\tilde{a}^1A_1$, $\tilde{b}^1B_1$, and $\tilde{c}^1A_1$) composed of the $2p_\sigma^2 2p_\pi^0$, $2p_\sigma^1 2p_\pi^1$, and $2p_\sigma^0 2p_\pi^2$ electronic configurations, respectively (see Scheme 1). One 2s(N) lone electron pair can find its way to the empty $2p_\sigma$ orbital of the $\tilde{c}^1A_1$ CH_2 state to form a planar H_2CN_2 structure of C_{2v} symmetry,[28,29] while π back donation from the doubly occupied CH_2 $2p_\pi$ orbital to the empty π^* N_2 orbital is realized at the same time (see Scheme 2). The addition of a second CH_2 entity (H_2CN_2 + CH_2) is expected to follow a similar mechanism in order to yield a C_{2v} $H_2CN_2CH_2$ structure with the two CH_2 planes being perpendicular to each other. Scheme 3 is depicting the vbL diagram for this mechanism.

Our calculations reveal that this C_{2v} structure is not the global minimum of the system but a second order saddle point moving toward methanol azine or formaldazine, denoted as $H_2C{=}N{-}N{=}CH_2(\tilde{X}^1A_g)$ to be distinguished from

Scheme 1. Electronic Structure of the Lowest Electronic States of Methylene

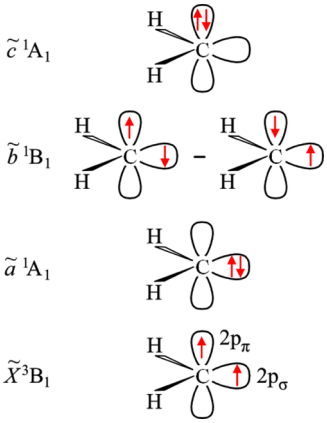

Scheme 2. vbL Diagram Describing Bonding in Diazomethane

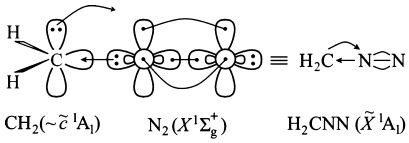

Scheme 3. vbL Diagram Describing Bonding in $H_2CN_2CH_2$

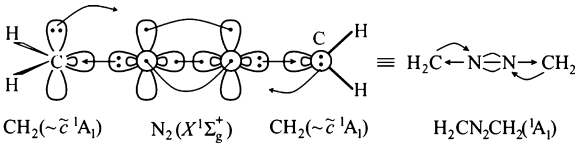

$H_2CN_2CH_2$ (C_{2v} structure). N_2 appears to be activated in the former case. The stability, geometry (C_{2h} point group), and vibrational features of formaldazine were first studied theoretically four decades ago.[30−32] This C_{2v} to C_{2h} structural transformation is barrier-free, and it is accompanied by an electronic structure reorganization. The two N_2 π bonds break, while at the same time, one σ and one π bond are created with each CH_2 moiety. Another way to see the bonding mechanism is through the simultaneous attack of two ground ($\tilde{X}^3B_1$)-state methylene moieties to the excited $^5\Sigma_g^+$ N_2 state, which results into the formation of σ and π covalent bonds (see Scheme 4). This picture suggests in situ access to a highly excited N_2 in an adiabatic manner.

The abovementioned considerations are explained in more detail supported by our quantum chemical calculations. To this end, full PEPs have been constructed for each reaction step. To keep these calculations manageable, we initially use CH_2. At the end, intermediates and transition states are located for the model persistent carbene, $((CH_3)_3C)_2C$.

Scheme 4. vbL Diagram Describing Bonding in $H_2C{=}N{-}N{=}CH_2$

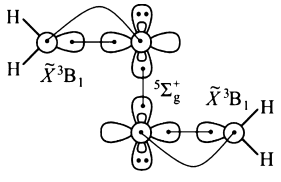

DOI: 10.1021/acs.jpcc.9b05124
J. Phys. Chem. C 2019, 123, 21548−21553

We start from the reaction of N_2 with CH_2. In the case of the N_2 + CH_2 planar approach (see Scheme 2 and Figure 1), the

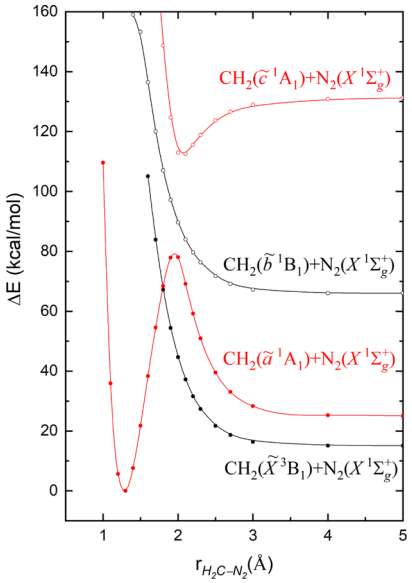

Figure 1. MRCI + Q/cc-pVTZ potential energy curves of the planar (C_{2v}) CH_2 + N_2 attack.

ground state of diazomethane dissociates to $CH_2(\tilde{a}^1A_1)$ + N_2 but arises from the $CH_2(\tilde{c}^1A_1)$ + N_2 channel through an avoided crossing with the $CH_2(\tilde{a}^1A_1)$ asymptotic limit. The CCSD(T)/cc-pVTZ equilibrium molecular parameters of the planar $\tilde{X}^1A_1$ diazomethane state are r_e(NN) = 1.143 Å, r_e(CN) = 1.303 Å, r_e(CH) = 1.075 Å, and ∠HCH = 125.2°. Through the σ and π back donation (see Scheme 2), the NN bond length increases by 0.039 Å with respect to the length in free N_2 ($X^1\Sigma_g^+$; r_e = 1.104 Å at the same level of theory).

Exactly the same mechanism prevails when another CH_2 attacks the other end of diazomethane. The empty $2p_\sigma$ carbon orbital facilitates the formation of a second σ dative bond. For this reason, the PEPs of Figure 2 are qualitatively similar to those of Figure 1. The CCSD(T)/cc-pVTZ equilibrium molecular parameters of the $^1A_1(C_{2v})$ $H_2CN_2CH_2$ structure are r_e(NN) = 1.185 Å, r_e(CN) = 1.280 Å, r_e(CH) = 1.085 Å, and ∠HCH = 120.6° (see also the Supporting Information). The N−N bond length (r_e = 1.185 Å; CCSD(T)/cc-pVTZ) is now found longer by 0.081 Å with respect to free N_2, which is twice the elongation distance (≈0.039 × 2) observed in $H_2CN_2(\tilde{X}^1A_1)$. The C−N distance shortens by 0.02 Å with respect to the one in diazomethane. The CCSD(T)/cc-pVTZ binding energy (D_e = 53.3 kcal/mol) of the $\tilde{X}^1A_1(C_{2v})$ $H_2CN_2CH_2$ structure with respect to $H_2CN_2(X^1A_1)$ + $CH_2(X^3B_1)$ is substantially larger than the binding energy (D_e = 29.6 kcal/mol) of $H_2CN_2(X^1A_1)$ with respect to $N_2(X^1\Sigma_g^+)$ + $CH_2(X^3B_1)$. All three observations suggest a synergistic effect of the two CH_2 moieties.

The lowest singlet spin PEP of Figures 1 and 2 indicate that the N_2 + CH_2 and H_2CN_2 + CH_2 reactions suffer from a substantial activation energy barrier. Looking at the PEPs for the perpendicular attack of N_2 to CH_2 (∠NCX of 90°; X is the middle point between the two H atoms of CH_2) or the subsequent perpendicular addition of H_2CN_2 to another CH_2, we see that the reaction is actually spontaneous (see Figures 3 and S1 of Supporting Information). The minimum energy

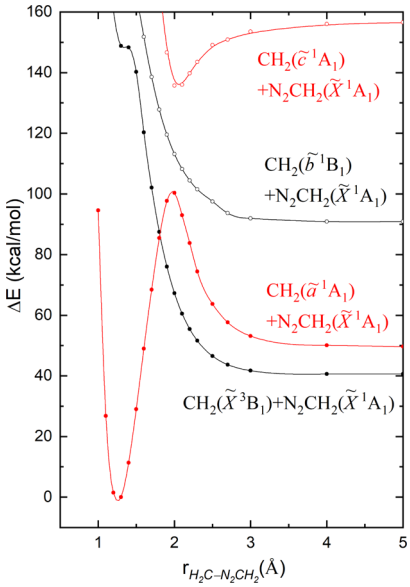

Figure 2. MRCI + Q/cc-pVTZ potential energy curves of the planar (C_{2v}) H_2CN_2 + CH_2 attack.

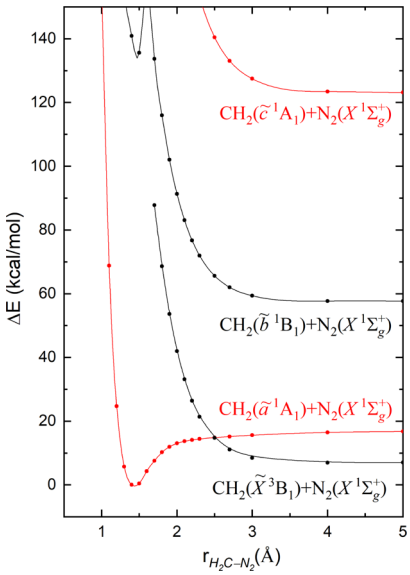

Figure 3. MRCI + Q/cc-pVTZ potential energy curves of the perpendicular CH_2 + N_2 attack.

structure dissociates smoothly to its adiabatic limit without any energy barrier. The vbL diagram of Scheme 5 can explain the observed morphology; the electron pair of N_2 is donated readily to the empty $2p_\pi$ orbital of $CH_2(\tilde{a}^1A_1)$. Optimization of the attack angle (∠NCX) at every C−N distance, that is, along the reaction coordinate of Figures 3 and S1, transforms the PEPs to the ones of Figures 4 and S2, where the minimum

Scheme 5. vbL Diagram Describing the Perpendicular Attack of N_2 to CH_2

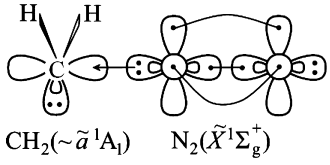

DOI: 10.1021/acs.jpcc.9b05124
J. Phys. Chem. C 2019, 123, 21548−21553

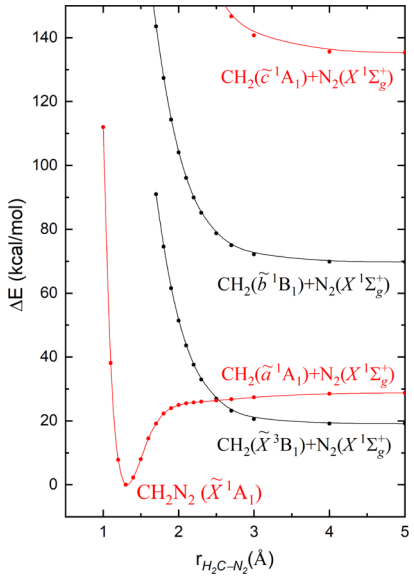

Figure 4. MRCI + Q/cc-pVTZ potential energy curves of the CH_2 + N_2 attack after optimizing the attack angle at every C−N distance.

energy curve (in red) connects the ground-state global minimum with its adiabatic limit in a barrier-free fashion. Our results for CH_2 + N_2 agree with Mavridis and co-workers,[28,33] and the exact same observation is seen here for H_2CN_2 + CH_2: N_2 or H_2CN_2 approach CH_2 first with a ∠NCX of 90° and gradually drops to 0° as they come closer to CH_2 bypassing the energy barrier.

The formed C_{2v} structure $H_2CN_2CH_2$ is not the global minimum of the system, but a second order saddle point with two imaginary frequencies (see the Supporting Information) evolving readily to the ground state of C_{2h} symmetry. Figure 5 contains the PEP for this transformation as a function of the two NNC angles that are kept equal at every single point of the reaction coordinate. The CCSD(T)/cc-pVTZ equilibrium molecular parameters of the $\tilde{X}^1A_g(C_{2h})$ CH_2═N−N═CH_2 state are r_e(NN) = 1.428 Å, r_e(CN) = 1.280 Å, r_e(CH) = 1.084/1.089 Å, ∠NNC = 110.3°, and ∠HCH = 120.4°. These values support that a σ-bond between two N atoms and a double bond between C and N.

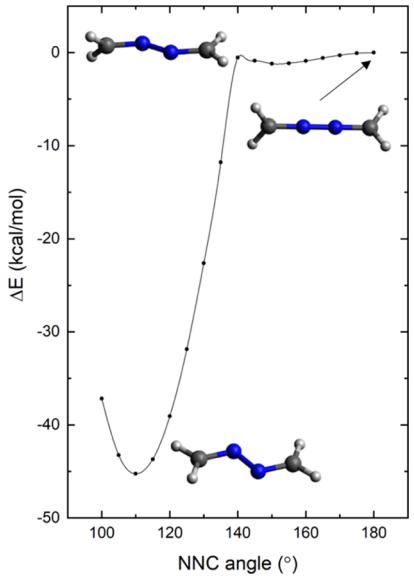

Figure 5. CCSD(T)/cc-pVTZ potential energy curve for the C_{2v} to C_{2h} structural transformation of $H_2CN_2CH_2$ to H_2C═N−N═CH_2.

To further support this picture, we formed the PEP pertaining to the attachment of two CH_2═N radicals. Its ground state is of $\tilde{X}^2B_2$ symmetry with the unpaired electron residing in an N(2p) orbital lying on the molecular H_2CN plane perpendicularly to the π_{CN} bond (see Scheme 4). The two unpaired electrons form readily a single bond as indicated by the PEP of Figure 6. Additionally, the spatial arrangement of the unpaired electrons in H_2C═N facilitates the formation of a C_{2h} global minimum.

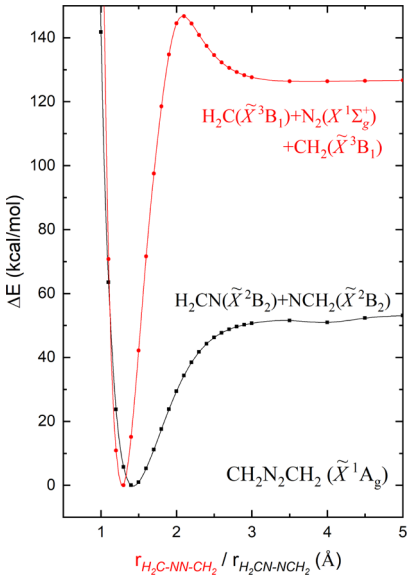

Figure 6. MRCI + Q potential energy curves of the C_{2h} attack of two CH_2 units to N_2 (red line) and of the C_{2h} interaction of two CH_2N radicals (black line).

Overall, the reaction $CH_2(\tilde{a}^1A_1)$ + $N_2(X^1\Sigma_g^+)$ + $CH_2(\tilde{a}^1A_1)$ leading to H_2C═N−N═CH_2 is barrier-free. Considering the ground-state fragments $CH_2(\tilde{X}^3B_1)$ + $N_2(X^1\Sigma_g^+)$ + $CH_2(\tilde{X}^3B_1)$, the synchronous approach of two $CH_2(\tilde{X}^3B_1)$ units to N_2 proceeds through a barrier of ∼20 kcal/mol (see the red line of Figure 6). The spin coupling of the two $CH_2(\tilde{X}^3B_1)$ units can generate a singlet spin state, and therefore, this path is part of the lowest singlet spin potential energy surface (PES). However, the stepwise reaction going through $CH_2(\tilde{X}^3B_1)$ + $N_2(X^1\Sigma_g^+)$ and $H_2CN_2(\tilde{X}^1A_1)$ + $CH_2(\tilde{X}^3B_1)$ corresponds to reactants of triplet spin symmetry. The passage through some conical intersection (CI) from the lowest energy triplet PES of the reactants to the lowest energy singlet PES of the products (H_2CN_2 and H_2C═N−N═CH_2) is necessary. Figures 3 and S1 provide an approximate position of these CIs and an estimate of the required energy to go through. In both cases, the singlet and triplet PEPs cross at around r_{CN} = 2.5 Å. Because this distance is quite long, the ∠NCX angle of the actual CI should be around 90°. The energy difference between the reactants and the crossing is less than 10 kcal/mol in either case, and it will be even lower if the optimal CI is found. Conclusively, the stepwise and not the synchronous reaction of the ground-state fragments provide the lowest energy path with a minimal energy barrier of less than 10 kcal/mol.

DOI: 10.1021/acs.jpcc.9b05124
J. Phys. Chem. C 2019, 123, 21548−21553

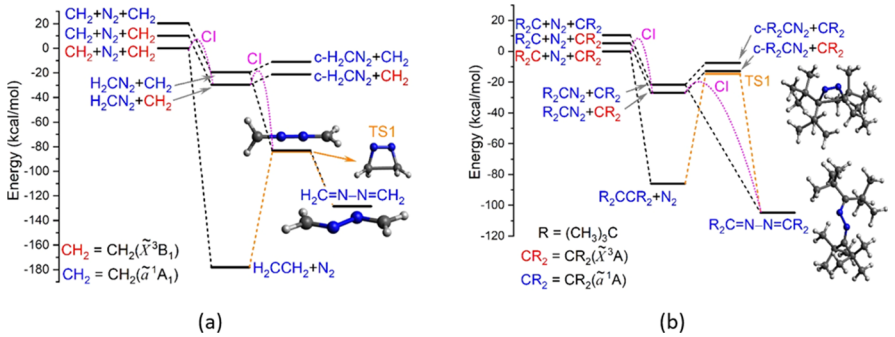

Figure 7. Energy landscape for (a) the $CH_2 + N_2 + CH_2$ and (b) the $CR_2 + N_2 + CR_2$ reactions, R = $(CH_3)_3C$. The CI positions are estimated from Figures 3 and S1; see text.

The complete energy landscape is presented in Figure 7a. To summarize, the ground state of $H_2CN_2CH_2$ is formed in three ways: the barrier-free sequential reaction of two $CH_2(^1A_1)$ units with N_2, the sequential reaction of two $CH_2(^3B_1)$ to N_2 units via CIs, and the route going through the formation of ethene and TS1, which connects $C_2H_4 + N_2$ with $H_2C{=}N{-}N{=}CH_2$. Ethene is the product of CH_2 diamerization and provides the most stable intermediate. The higher energy cyclic H_2CN_2 (c-H_2CN_2) species of the $CH_2 + N_2$ reaction is also included.

The picture changes considerably in the case of persistent carbene (R_2C) with R = $(CH_3)_3C$. The energy landscape shares identical features with that of methylene (CH_2), suggesting a very similar mechanism, but the dimer of the model carbene (R_2CCR_2) is not stable compared to the N_2 association product ($R_2C{=}N{-}N{=}CR_2$); see Figure 7b. Also, we could not locate the C_{2v} $R_2CN_2CR_2$ structure. Future work will focus on locating persistent carbenes with the singlet spin ground state (if possible), for which the stability of their dimer and the energy barrier separating it from $R_2C{=}N{-}N{=}CR_2$ are smaller.

4. CONCLUSIONS

Using quantum chemical approaches, we report the activation process of the triply bonded N_2 system by means of persistent carbene pairs. With the purpose to elucidate the mechanism in electronic structure terms, we constructed PEPs and monitored the electronic structure reorganization for every reaction step. We demonstrated that carbenes act synergistically exactly as FLPs and are capable to act as a Lewis acid and base at the same time (Schemes 2 and 3), enabling the cleavage of multiple bonds. To simplify our study, we currently employed the model carbenes CH_2 and $((CH_3)_3C)_2C$. A more systematic exploration of a variety of carbene pairs and the activation of different chemical bonds, such as CO or CO_2, will be attempted in the near future. We hope that our results will inspire the experimental community and lead to practical applications.

■ ASSOCIATED CONTENT

Supporting Information

The Supporting Information is available free of charge on the ACS Publications website at DOI: 10.1021/acs.jpcc.9b05124.

Additional PEPs for the oblique approach of H_2CN_2 to CH_2; Cartesian coordinates and harmonic vibrational frequencies at CCSD(T)/cc-pVTZ for methylene and B3LYP-D3/cc-pVTZ for $((CH_3)_3)_2C$; optimal structures; exact energy values; and T_1 diagnostics for the CCSD calculations (PDF)

■ AUTHOR INFORMATION

Corresponding Authors

*E-mail: kalemos@chem.uoa.gr (A.K.).
*E-mail: emiliord@auburn.edu (E.M.).

ORCID

Shahriar N. Khan: 0000-0002-8913-8430
Apostolos Kalemos: 0000-0002-1022-0029
Evangelos Miliordos: 0000-0003-3471-7133

Notes

The authors declare no competing financial interest.

■ ACKNOWLEDGMENTS

S.N.K. and E.M. are indebted to Auburn University (AU) for financial support. This work was completed with resources provided by the AU Hopper Cluster.

■ REFERENCES

(1) Huber, K. P.; Herzberg, G. Constants of Diatomic Molecules (data prepared by J. W. Gallagher and R. D. Johnson, III). In *NIST Chemistry WebBook, NIST Standard Reference Database Number 69*; Linstrom, P. J., Mallard, W. G., Eds.; National Institute of Standards and Technology: Gaithersburg MD, retrieved November 23, 2018; p 20899.

(2) Kalemos, A.; Ariyarathna, I. R.; Khan, S. N.; Miliordos, E.; Mavridis, A. "Hypervalency" and the chemical bond. *Comput. Theor. Chem.* **2019**, *1153*, 65−74.

(3) Allen, A. D.; Senoff, C. V. Nitrogenopentammineruthenium(II) Complexes. *Chem. Commun.* **1965**, 621−622.

(4) Clouston, L. J.; Bernales, V.; Carlson, R. K.; Gagliardi, L.; Lu, C. C. Bimetallic Cobalt-Dinitrogen Complexes: Impact of the Supporting Metal on N_2 Activation. *Inorg. Chem.* **2015**, *54*, 9263−9270.

(5) Fryzuk, M. D. More Can Be Better in N_2 Activation. *Science* **2013**, *340*, 1530.

(6) Fryzuk, M. D. N_2 coordination. *Chem. Commun.* **2013**, *49*, 4866−4868.

(7) Howard, J. B.; Rees, D. C. Structural Basis of Biological Nitrogen Fixation. *Chem. Rev.* **1996**, *96*, 2965−2982.

(8) Melen, R. L. A Step Closer to Metal-Free Dinitrogen Activation: A New Chapter in the Chemistry of Frustrated Lewis Pairs. *Angew. Chem., Int. Ed.* **2018**, *57*, 880−882.

(9) Shaver, M. P.; Fryzuk, M. D. Activation of Molecular Nitrogen: Coordination, Cleavage and Functionalization of N_2 Mediated By Metal Complexes. *Adv. Synth. Catal.* **2003**, *345*, 1061−1076.

(10) Siedschlag, R. B.; Bernales, V.; Vogiatzis, K. D.; Planas, N.; Clouston, L. J.; Bill, E.; Gagliardi, L.; Lu, C. C. Catalytic Silylation of

DOI: 10.1021/acs.jpcc.9b05124
J. Phys. Chem. C 2019, 123, 21548−21553

Dinitrogen with a Dicobalt Complex. *J. Am. Chem. Soc.* **2015**, *137*, 4638−4641.
(11) Appl, M. Ammonia. *Ullmann's Encyclopedia of Industrial Chemistry*; Wiley-VCH: Weinheim, 2006.
(12) Stephan, D. W. "Frustrated Lewis pairs": a concept for new reactivity and catalysis. *Org. Biomol. Chem.* **2008**, *6*, 1535−1539.
(13) Stephan, D. W. Frustrated Lewis Pairs: From Concept to Catalysis. *Acc. Chem. Res.* **2015**, *48*, 306−316.
(14) Stephan, D. W. Frustrated Lewis Pairs. *J. Am. Chem. Soc.* **2015**, *137*, 10018−10032.
(15) Berkefeld, A.; Piers, W. E.; Parvez, M. Tandem Frustrated Lewis Pair/Tris(pentafluorophenyl)borane-Catalyzed Deoxygenative Hydrosilylation of Carbon Dioxide. *J. Am. Chem. Soc.* **2010**, *132*, 10660−10661.
(16) Stephan, D. W. Frustrated Lewis Pairs: A New Strategy to Small Molecule Activation and Hydrogenation Catalysis. *Dalton Trans.* **2009**, 3129−3136.
(17) Welch, G. C.; Juan, R. R. S.; Masuda, J. D.; Stephan, D. W. Reversible, Metal-Free Hydrogen Activation. *Science* **2006**, *314*, 1124.
(18) Tang, J.; Gao, X. J.; Tang, H.; Zeng, X. Dioxygen Activation with Stable N-heterocyclic Carbenes. *Chem. Commun.* **2019**, *55*, 1584−1587.
(19) Frey, G. D.; Lavallo, V.; Donnadieu, B.; Schoeller, W. W.; Bertrand, G. Facile Splitting of Hydrogen and Ammonia by Nucleophilic Activation at a Single Carbon Center. *Science* **2007**, *316*, 439.
(20) Légaré, M.-A.; Rang, M.; Bélanger-Chabot, G.; Schweizer, J. I.; Krummenacher, I.; Bertermann, R.; Arrowsmith, M.; Holthausen, M. C.; Braunschweig, H. The Reductive Coupling of Dinitrogen. *Science* **2019**, *363*, 1329.
(21) Légaré, M.-A.; Bélanger-Chabot, G.; Dewhurst, R. D.; Welz, E.; Krummenacher, I.; Engels, B.; Braunschweig, H. Nitrogen fixation and reduction at boron. *Science* **2018**, *359*, 896.
(22) Townsend, J.; Braunscheidel, N. M.; Vogiatzis, K. D. Understanding the Nature of Weak Interactions between Functionalized Boranes and N_2/O_2, Promising Functional Groups for Gas Separations. *J. Phys. Chem. A* **2019**, *123*, 3315−3325.
(23) Bourissou, D.; Guerret, O.; Gabbaï, F. P.; Bertrand, G. Stable Carbenes. *Chem. Rev.* **2000**, *100*, 39−92.
(24) Hopkinson, M. N.; Richter, C.; Schedler, M.; Glorius, F. An Overview of N-heterocyclic Carbenes. *Nature* **2014**, *510*, 485.
(25) Werner, H.-J.; Knowles, P. J.; Knizia, G.; Manby, F. R.; Schütz, M.; Celani, P.; Györffy, W.; Kats, D.; Korona, T.; Lindh, R.; et al. *MOLPRO*, version 2015.1, 2015.
(26) Frisch, M. J.; Trucks, G. W.; Schlegel, H. B.; Scuseria, G. E.; Robb, M. A.; Cheeseman, J. R.; Scalmani, G.; Barone, V.; Petersson, G. A.; Nakatsuji, H.; et al. *Gaussian 16*; Gaussian, Inc.: Wallingford CT, 2016.
(27) Chen, B.; Rogachev, A. Y.; Hrovat, D. A.; Hoffmann, R.; Borden, W. T. How to Make the $\sigma^0\pi^2$ Singlet the Ground State of Carbenes. *J. Am. Chem. Soc.* **2013**, *135*, 13954−13964.
(28) Papakondylis, A.; Mavridis, A. A Theoretical Investigation of the Structure and Bonding of Diazomethane, CH_2N_2. *J. Phys. Chem. A* **1999**, *103*, 1255−1259.
(29) Papakondylis, A.; Mavridis, A. Accurate Structural Parameters and Binding Energy of the X^1A_1 State of Diazomethane Through Coupled-Cluster Calculations. *Chem. Phys. Lett.* **2014**, *600*, 103−105.
(30) Ogilvie, J. F.; Cole, K. C. Vibrational Spectra and Conformation of Methanal Azine. *Spectrochim. Acta, Part A* **1971**, *27*, 877−895.
(31) Ogilvie, J. F. A Spectroscopic Study of the Photodecomposition of Diazomethane. *Photochem. Photobiol.* **1969**, *9*, 65−89.
(32) Ogilvie, J. F.; Cyvin, S. J.; Cyvin, B. N. Harmonic Force Fields and Mean Amplitudes of Vibration for Some Molecules Containing Nitrogen: Methanal Azine. *J. Mol. Struct.* **1973**, *18*, 285−293.
(33) Kerkines, I. S. K.; Cársky, P.; Mavridis, A. A Multireference Coupled-Cluster Potential Energy Surface of Diazomethane, CH_2N_2. *J. Phys. Chem. A* **2005**, *109*, 10148−10152.

DOI: 10.1021/acs.jpcc.9b05124
J. Phys. Chem. C 2019, 123, 21548−21553